

Sophie Gröger, Marco Weißgerber (Hrsg.)

## **XIV. Internationales Oberflächenkolloquium**

XIV. International Colloquium on Surfaces

30.01.-01.02.2017

an der Technischen Universität Chemnitz

### **Tagungsband**



TECHNISCHE UNIVERSITÄT  
CHEMNITZ

**Universitätsverlag Chemnitz  
2017**

## **Impressum**

### **Bibliografische Information der Deutschen Nationalbibliothek**

Die Deutsche Nationalbibliothek verzeichnet diese Publikation in der Deutschen Nationalbibliografie; detaillierte bibliografische Angaben sind im Internet über <http://dnb.d-nb.de> abrufbar.

Titelgrafik: Sophie Gröger  
Satz/Layout: Marco Weißgerber

Technische Universität Chemnitz/Universitätsbibliothek  
**Universitätsverlag Chemnitz**  
09107 Chemnitz  
<http://www.tu-chemnitz.de/ub/univerlag>

### **Herstellung und Auslieferung**

readbox unipress  
Am Hawerkamp 31  
48155 Münster

readbox unipress ist eine Marke der  
readbox publishing GmbH  
Ruhrallee 9  
44139 Dortmund  
<http://unipress.readbox.net>

ISBN 978-3-96100-006-7

<http://nbn-resolving.de/urn:nbn:de:bsz:ch1-qucosa-215831>

---

## INHALTSVERZEICHNIS

<b>Funktion und Geometrie - Betrachtungen an der Oberfläche</b>	<b>1</b>
Gröger, S.; Weißgerber, M.; Hofmann, R.	
<b>Form removal aspects on the waviness parameters for steel in automotive applications: Fourier filtering vs. polynomial regression</b>	<b>11</b>
Vermeulen, M.; Balabane, M.; Mallé, C.	
<b>Einfluss des Fertigungsprozesses auf die Feingestalt und Funktionalität von Bauteiloberflächen und deren Bewertung</b>	<b>21</b>
Schneider, J.; Schmidt, T.; Edelman; J.; Putz, M.	
<b>Funktionale 3D-Oberflächencharakterisierung der Zylinderlaufbahn in der Automobilindustrie</b>	<b>31</b>
Machleidt, T.; Lucht, C.; Schwannecke, H.-C.; Flores, G.; Besch, D.	
<b>Geometrieanforderungen bei metallischen Bipolarplatten in PEM-Brennstoffzellen</b>	<b>41</b>
Lötsch, K.; Jendras, P.; Härtel, S.; von Unwerth, T.	
<b>Bezüge und Toleranzen – Spannungsfeld Norm und reale Anwendung</b>	<b>53</b>
Bohn, M.; Hetsch, K.	
<b>Wie vergleichbar ist die geometrische Tolerierung nach ISO und ASME?</b>	<b>61</b>
Schönberg, B.	
<b>Integrative Messtechnik - Neuentwicklungen in der automatisierten Rauheits- und Konturmesstechnik</b>	<b>69</b>
Klöden, R.	
<b>Schneller in der Oberflächenmesstechnik: Aperturkorrelation und Koordinatenmessgeräteintegration</b>	<b>79</b>
Imkamp, D; Drescher, V.	
<b>3D-Oberflächensensor für den industriellen Einsatz mit sensornaher Verarbeitungskette auf FPGA-Basis</b>	<b>87</b>
Schwannecke, H.-C.; Wenzel, K.; Machleidt, T.	
<b>Moderne Oberflächenmessung: Gestalt und Gestaltabweichungen</b>	<b>93</b>
Kedziora, H.-J.; Meyer, M.; Volk, R.	
<b>Einflüsse der Oberflächenstruktur auf die Streuung von Rauheitskennwerten: Praxisrelevante Untersuchungen</b>	<b>105</b>
Rief, S.; Seewig, J.; Hüser, D.	

---

---

<b>Eignungsprüfung konfokaler Sensoren zur Rauheitsmessung</b> Schwarzer, F.; Volk, R.	<b>115</b>
<b>Warum brauchen wir in der Oberflächenmesstechnik eine Norm für Oberflächendefekte auf Kalibriernormalen?</b> Rubert, P.	<b>123</b>
<b>Weiterentwickelte Ansätze zur Charakterisierung von Kanten an Schneidwerkzeugen und Werkstücken</b> Uhlmann, E.; Roßkamp, S.; Eulitz, A.	<b>131</b>
<b>Komplexe Geometrien mit nur einem optischen Messsystem vermessen</b> Bauer, C.; Hahne, S.	<b>145</b>
<b>Kalibrierung kleiner Radien mittels Tastschnittgerät</b> Thomsen-Schmidt, P.; Brand, U.	<b>155</b>
<b>Automatische 3D-Auswertung der Schneidkantenqualität durch Fokus-Variation</b> Danzl, R.; Helmlí, F.	<b>165</b>
<b>Bestimmung der 2D-Geometrie von Silizium-Mikrotastern</b> Langfahl-Klabes, J.; Doering, L.; Brand, U.	<b>175</b>
<b>Herausforderungen des Einsatzes unterschiedlicher Messbezugssysteme in der Prozesskette Aluminium-Struktur-gussbauteilbearbeitung</b> Von Kuepach, S.; Wagensoener, M.; Roeren, S.	<b>185</b>
<b>Prozessstabilisierung, Effizienzsteigerung und Technologieweiterentwicklung durch automatisierte Oberflächenfehlererkennung im Rahmen der Gesamtprozesskette Aluminium-Strukturbauteile – Einführung eines Würfelmodells zur Einordnung von Erkenntnissen</b> Wagensoener, M.; von Kuepach, S.; Roeren, S.	<b>191</b>

---

# FORM REMOVAL ASPECTS ON THE WAVINESS PARAMETERS FOR STEEL SHEET IN AUTOMOTIVE APPLICATIONS: FOURIER FILTERING VERSUS POLYNOMIAL REGRESSION

**Vermeulen Michel<sup>1,2</sup>, Balabane Mikhael<sup>3</sup>, Mallé Céline<sup>4</sup>**

<sup>1</sup> Ghent University, Mechanical Construction and Production, michel.vermeulen@ugent.be

<sup>2</sup> OCAS / ArcelorMittal Global R&D Ghent, michel.vermeulen@arcelormittal.com

<sup>3</sup> Université de Paris13, Dept. de Math., Inst. Galilee, balabane@math.univ-paris13.fr

<sup>4</sup> ArcelorMittal Global R&D, Maizière les Metz, celine.malle@arcelormittal.com

*Abstract: Premium car makers attach great importance to the visual appearance of the painted car skin as an indication of product quality. The “orange peel” phenomenon constitutes a major problem here. It is not only depending on the paint’s chemical composition and application method, but also on possible waviness components in the sheet substrate. Therefore one is searching hard for a valuable waviness parameter to quantify the substrate’s fitness for purpose. A technically emerging problem is how to remove the form from the measured signal, which is indeed not significant to the orange peel phenomenon. This paper will compare two commonly used approaches: i.e. Fourier filtering versus polynomial regression and will reveal and quantify some common aspects in terms of wavelengths.*

ROUGHNESS, WAVINESS, FORM REMOVAL, FOURIER, LEGENDRE

## 1. INTRODUCTION: INDUSTRIAL RELEVANCE

Cars are sold in the showroom and emotion often comes before rational reasoning. The automotive industry dedicates numerous studies to analyse the consumer behaviour when purchasing a new car. The perceived quality of a car is judged within the first 10 minutes of the “encounter”. While the outer skin of the car constitutes a large area of “interface to the consumer”, the exterior paint plays a dominant role here, see Figure 1. [Gerhardt, 2013]

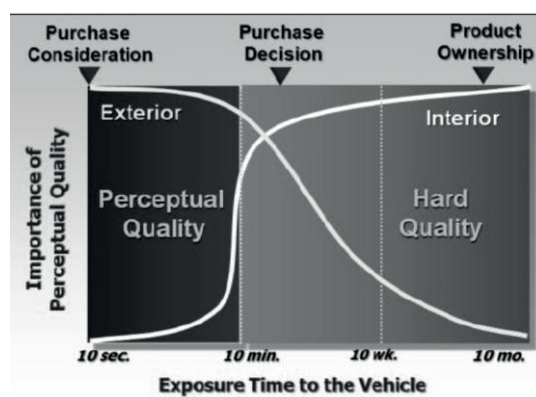


Fig. 1: Perception of Product Quality and the role of the Exterior Appearance [Gerhardt, 2013]

Carmakers set up special test rigs to assess the visual perception of painted panels and are trying to establish the relation between personal judgments and the quantitative measurements on the painted surface [Dauser, 2013]. In such a setup, a straight line source is reflected towards the panels, and the operator must decide on his preference, based on the distortion of the reflected line source, see Figure 2, left.

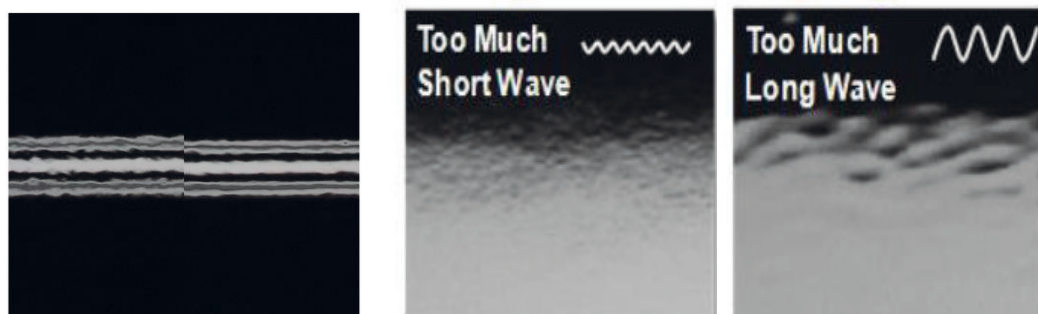


Fig. 2: Left: Reflection of straight line light on two panels with different quality [Dauser, 2013], Right: Discriminating short and long waves in a painted panel [Gerhardt, 2013]

But very soon, one is confronted with the problem of discriminating the scale of this distortion, see Figure 2, right. Moreover, there are still some debates on how to correlate the paint measurements with the visual perception, but one generally accepts that the longer waviness components are quite detrimental and cause the so called “orange peel” aspect, as being in the range of  $\sim 1$  mm up to 10 or even 12 mm: [Gerhardt, 2013] and [Schneider, 2013].

Extensive research has been performed in the past and is still on-going on how the topography of the subsequent layers is evolving. It is obvious that the chemical paint composition and the paint process are dominating the formation of the top layer when painting a sheet panel. It is found that fine surface structures are easily levelled away due to surface tension effects during curing. Coarser structures however cannot be hidden completely or are even emphasized, especially on vertically painted panels. Research on this topic is twofold. First, one has the purely experimental work based on 3D-profiling as reported in e.g. [Meseure, 1996], Figure 3 and in [Deutscher, 2003] or on 2D-profiling, e.g. Figure 4 [Kurzynski, 2015]. It finally leads to fundamental modelling of the physical phenomena of wetting, gravity and rheology-effects, curing, etc., as is done in e.g. [Schneider, 2013].

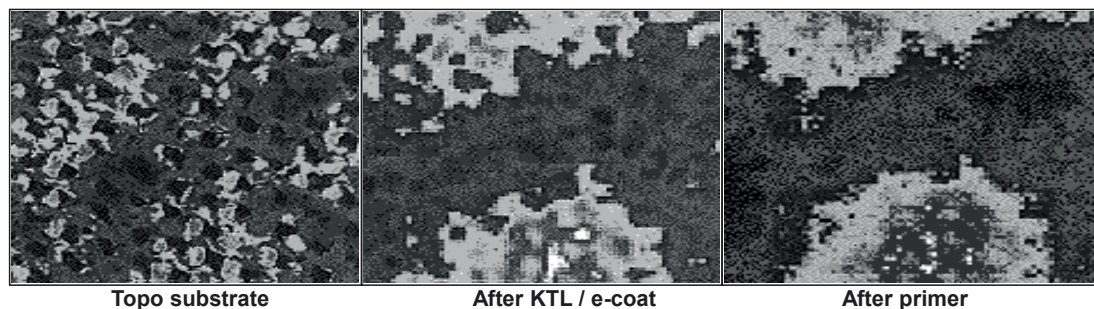


Fig. 3: Levelling effect of subsequent layers [Meseure, 1996]

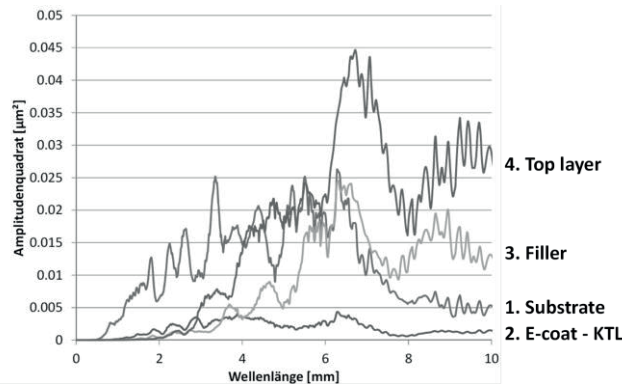


Fig. 4: Evolution of the power spectrum of subsequent layers during painting [Kurzynski, 2015]

During the last 5-10 years, environmental concerns have led to the use of water based paints, while weight and cost savings considerations brought up a reduction of layer thicknesses and even the omission of the primer layer. All these elements together tend to emphasize the importance of the substrate topography, see Figure 4 from [Kurzynski, 2015]. In this way steel producers are forced to guarantee on their products not only some strict roughness ranges (for both painting and stamping purposes, as per [EN10049, 2013]). These products also have to remain below a limit value of waviness in order to minimize the effect of the unpainted substrate topography on a potential “orange peel” appearance on the final painted car skin.

## 2. PROBLEM DEFINITION: TOWARDS A WAVINESS PARAMETER?

The paint process essentially is a 3D phenomenon, and profound (modelling) research should be validated by 3D measurements. As indicated before, the area to be measured must be quite large, due to the wavelength range to be covered and the fact that one needs 3 or preferably 5 times this length for an adequate spectral analysis. One rapidly arrives at square or rectangular areas of 30 to 50 mm size. Tactile 3D-profiling instruments are slow due to limitations in traversing speed. Faster optical instruments are becoming more affordable nowadays. They can acquire 3D areas in one single scan, but the area of a “single shot” is limited: indeed intending for a high resolution drastically reduces the field of view. Modern optical instruments do offer stitching possibilities. However, harmful waviness components have amplitudes in the order of 0.1 to 1  $\mu\text{m}$  while the roughness range is up to 50 times larger. It is clear that one has to be very careful with stitching - either software or hardware stitching - in order to not introduce any “artificial waviness” that is physically not present in the real surface.

For measurements in daily and possibly shop floor conditions, one is still forced to rely on 2D measurements by profiling a set of (parallel) traces to reduce the variability of the resulting parameters. Even in 2D one has to be aware of the magnitude difference between waviness and roughness, i.e. only datum based traversing units can be used, both for tactile and optical point sensors.

Elaborating a waviness parameter, means treating the 2D measured profiles for removing the roughness and the form; see Figure 5. Indeed, as said before, roughness is virtually levelled away during the paint application and shouldn't affect the waviness parameter. Further, the general form of the sample is not a defect, and should be eliminated by means of a form removal procedure.

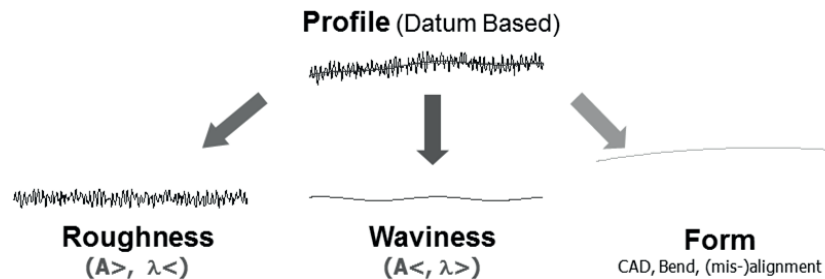


Fig. 5: Splitting the measured profile into roughness, waviness and form

Within the ISO TC213, current work on surface topography standardisation concentrates a lot on filtering and mainly on different variants of “splitting” roughness and waviness to be extracted from the raw measured data – both for profiles and surfaces. Little emphasis is given so far to the not less important problem of form removal, which is classified in general terms as a “F-operator”.

The analysis described hereafter originated within the VDEh-Arbeitskreis Rauheit during the elaboration of a guideline for the steel and automotive industry. Within this working group, first basic work was performed in a European Project CARSTEEL [Deutscher, 2009]. In this project a multitude of waviness parameters were compared as they were practised in former days. The CARSTEEL project resulted in a guideline [SEP1941, 2012] which includes the two remaining methods as they are used nowadays.

### 3. FORM REMOVAL

The SEP1941 describes the waviness parameters Wsa(1-5) and Wa0.8 and two different methods for form removal are included, see Figure 6.

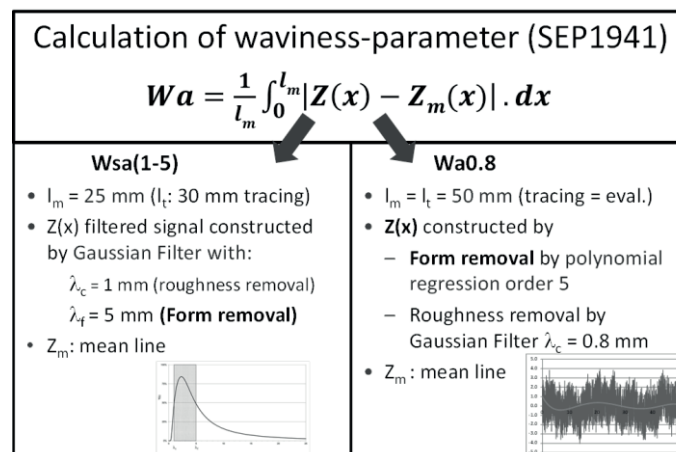


Fig. 6: Definition of Waviness Parameters Wsa(1-5) and Wa0.8 [SEP1941, 2012]

In addition to a difference in measuring length, one main difference is the way how form removal is performed: either Fourier (Gaussian) filtering or polynomial regression. A recently finished Project WAVENORM [Kurzynski, 2015] intended to acquire practical experience with both methods. In the following, differences and similarities will be investigated in more detail.

### 3.1 Fourier decomposition and form removal by Gaussian filtering

Before tackling the two above mentioned approaches, it is necessary to recall some basics in signal decomposition. In principle there are several methods, e.g. Fourier, wavelets, etc. Wavelet decomposition is used throughout the world of audio and video for data compression, but will not be discussed here.

Fourier decomposition is probably the best known. It is most popular in noise and vibration problems and was originally developed for time signals. It is however also vastly applied to 2D-profiles and even to 3D-surfaces. Fourier (°1768-°1830) demonstrated that any function of length  $Lt$  can be written as a sum of sine functions of well-defined frequencies, each with an amplitude  $b_n$  and a phase  $\varphi_n$ . If applied to a digital format with  $N$  samples within  $Lt$ , one gets:

$$z = f(x) = b_0 + \sum_{n=1}^{N/2} b_n \cdot \sin(2\pi f_n \cdot x + \varphi_n), \text{ with } f_n = n \cdot \Delta f \text{ and } \Delta f = 1/Lt \quad (1)$$

In surface topography, one is merely interested to use wavelengths i.s.o. frequencies; each component's wavelength is then:

$$\lambda_n = 1/f_n = Lt/n \quad (2)$$

A plot with the amplitudes  $b_n$  versus frequencies contains equally spaced frequency components. However if plotted versus wavelengths the gap between adjacent points is variable; especially the longer wavelengths are spaced quite far apart. As an example, the theoretical profile of the CARSTEEL Waviness gauge is used to demonstrate this effect, see Figure 7. The profile consists of a random roughness taken from a real sample, which is cut-off at 2.5 mm and 3 sine signals with amplitudes  $A$  and wavelengths  $\lambda$  of respectively: (i) S1:  $A = 0.7 \mu\text{m}$  &  $\lambda = 4.52 \text{ mm}$ , (ii) S2:  $A = 1.2 \mu\text{m}$  &  $\lambda = 3.31 \text{ mm}$  and (iii) S3:  $A = 0.8 \mu\text{m}$  &  $\lambda = 1.5 \text{ mm}$ . In addition a parabolic bow of  $30 \mu\text{m}$  is introduced, representing some bend as found in real samples.

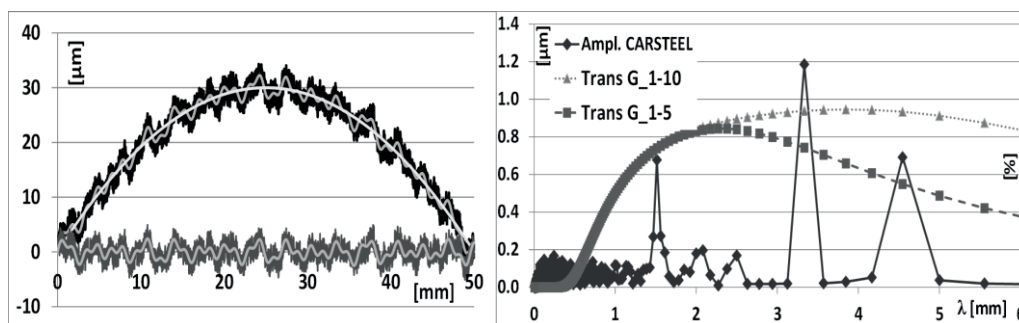


Fig. 7: Left: The theoretical CARSTEEL waviness Gauge profile; top curve includes a bow, Right: Amplitude versus wavelength with the transmission curves for Gaussian band filtering, according to SEP1941 but with two different cut-offs for the form removal

Remark that increasing the sampling rate or decreasing the spacing  $\Delta x$  between adjacent measured points (i.e. increase of  $N$ ), doesn't affect this variable spacing phenomenon. The only way to improve the resolution in the longer wavelength range is to increase the measurement length  $L_t$ . A measure that is pretty hard to implement in practice, as this would result in even longer measuring times and also in higher instrument costs.

Filtering a signal can then be performed by reducing or zeroing selected spectral components. In the surface topography community one commonly uses the Gaussian filter characteristic, given by its transmission curve for either low pass, high pass [ISO 16610-21, 2011] or even band pass filter as e.g. in [SEP1941, 2012]. The transmission curves are well described analytically in both references. For a band pass filter with a roughness cut-off  $\lambda_c$  and a form cut-off  $\lambda_f$ , equation (3) is given below with  $B_0$  and  $B_b$  being the amplitudes of respectively the original signal and of the band filtered components. The “cut-off wavelength” means the point where the transmission is exactly 50% and one uses the terms low and high from the wavelength point of view (and not in the frequency space).

$$B_b/B_0 = 2^{-(\lambda_c^2/\lambda^2)} \cdot [1 - 2^{-(\lambda_f^2/\lambda^2)}] \quad (3)$$

Note that reconstructing the filtered signal is readily possible, as only the amplitudes are reduced and the phase information remains unaffected. This eliminates phase distortion, as was found in the earliest and now out-dated analogue roughness devices.

### 3.2 Form removal by Polynomial regression

It's commonly known - although quite intuitive - that fitting a higher degree of polynomial will lead to a more “flexible” fit, which includes higher frequencies (or shorter wavelengths) to be subtracted from the raw data. However, in spite of being available in most software packages, little attention has been given until now to **quantify** these effects.

#### 3.2.1. “Pseudo transmission curves” for polynomial regression

A first somehow naïve attempt is described hereafter by building “pseudo transmission curves”. The aim is to get a first idea of how a classic polynomial regression behaves and whether there is some cut-off effect, when looking as from the Fourier point of view. Although we know that polynomial regression is not comparable to a Gaussian filtering, one nevertheless can try to establish “experimentally” a transmission curve. This has been done with the help of the same approach as used in system identification problems, see thereto the scheme of Figure 8. The system is “fed” with sine-signals of variable wavelength but constant amplitude, e.g. 1  $\mu\text{m}$ , similar to the “sweeping method” in system identification. Then either the Gaussian form filter is used or a polynomial regression is performed. The  $W_a$ -parameter is calculated solely based on the “filtered” profile, resulting in a set of  $W_a$ -values for various wavelengths. These are divided by the theoretical value  $W_{a\text{theo}} = 2A/\pi$ , being

independent of wavelength. From this, a “pseudo transmission curve” is built, see Figure 8, right.

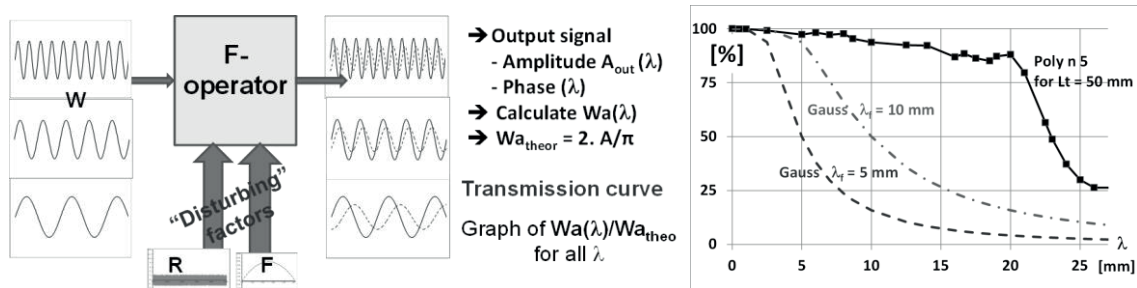


Fig. 8: Left: “Experimentally” building a transmission curve for polynomial regression, Right: Result for “Pseudo transmission curve” for polynomial regression order 5, compared with 2 Gaussian curves for  $\lambda_f = 5$  and 10 mm

### 3.2.2. Legendre polynomials

The use of Legendre polynomials is rooted in the geometric structure of signal processing, enabling a projection to replace the usual classic polynomial fitting, and hence resulting in a substantial gain of computing time and facilitating a straightforward interpretation in terms of wavelengths. Legendre (°1752-+1833) established a system of special polynomials, which are used in various scientific areas, e.g. quantum mechanics. They are commonly expressed in their normalised form, i.e. in the interval [-1, +1] for both x and  $P_n(x)$ . The equations for the first 5 polynomials, with their graphical representations are given in Figure 9. When analysing the normalised Legendre polynomials, one can easily identify “waves” with a wavelength, which is solely depending on the order n, i.e.  $2/(n-1)$ .

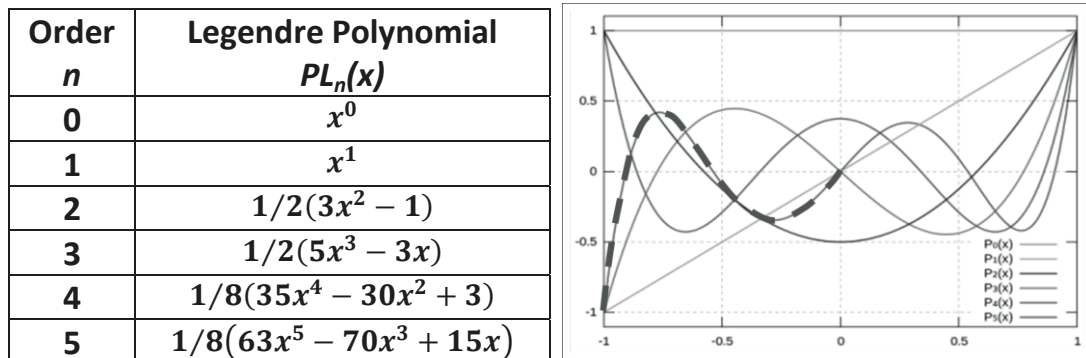


Fig. 9: Left: Legendre polynomials (order  $n = 0 - 5$ ), Right: graphical representation, with indicating one “wave” for  $PL_5$

### 3.2.3. Classic polynomial regression versus Legendre polynomial regression

It is interesting to look at the similarity between classic and Legendre polynomials ( $PL_n$ ): see equations resp. (4) and (5).

$$Z(x) = a_n x^n + \dots + a_3 x^3 + a_2 x^2 + a_1 x^1 + a_0 \quad (4)$$

$$Z(x) = A_n \cdot PL_n(x^*) + \dots + A_3 \cdot PL_3(x^*) + A_2 \cdot PL_2(x^*) + A_1 \cdot PL_1(x^*) + A_0 \quad (5)$$

There to, a rescaling is necessary for the Legendre polynomials from the interval  $[-1, +1]$  to the measured profile with interval  $[0, Lt]$ , using equation (6).

$$x^* = (2x - Lt)/Lt \quad (6)$$

This rescaling leads to adjust the cut-off wavelength for a measured profile into:

$$\lambda_{PL_n} = 2/(n - 1) \cdot Lt \quad \text{with } n > 1 \quad (7)$$

Introducing the full expressions of the Legendre polynomials in (5) and equalling the coefficients of the same power in both equations (4) and (5) yield the equations (8). For simplicity, only order 4 is written explicitly, but the general form is valid.

$$\begin{pmatrix} a_0 \\ a_1 \\ a_2 \\ a_3 \\ a_4 \end{pmatrix} = \begin{bmatrix} 1 & 0 & -1/2 & 0 & 3/8 \\ 0 & 1 & 0 & -3/2 & 0 \\ 0 & 0 & -3/2 & 0 & -30/8 \\ 0 & 0 & 0 & 5/3 & 0 \\ 0 & 0 & 0 & 0 & 34/8 \end{bmatrix} * \begin{pmatrix} A_0 \\ A_1 \\ A_2 \\ A_3 \\ A_4 \end{pmatrix} \quad (8a)$$

Or in general:

$$\{a_n\} = [M_n] * \{A_n\} \quad (8b)$$

Note that the Matrix  $M_n$  is only depending on the coefficients of the *normalised* Legendre polynomials. This means that with the help of a simple and unique transformation matrix (one for each order), one can swap from “classic” polynomials to the Legendre polynomials and vice-versa.

As seen above, one can allocate wavelengths to the Legendre polynomials, so the unique transformation enables to extend this feature to the classic polynomials. Each fit to another profile will yield other coefficients  $a_0 \dots a_n$  and  $A_0 \dots A_n$ , but the transformation matrix  $M_n$  remains unchanged, as it contains only the coefficients of the normalised Legendre polynomials. This means that the cut-off wavelength remains unaffected and **is only depending on the order of the polynomial fit AND the measuring length  $Lt$** . This is shown in Figure 10.

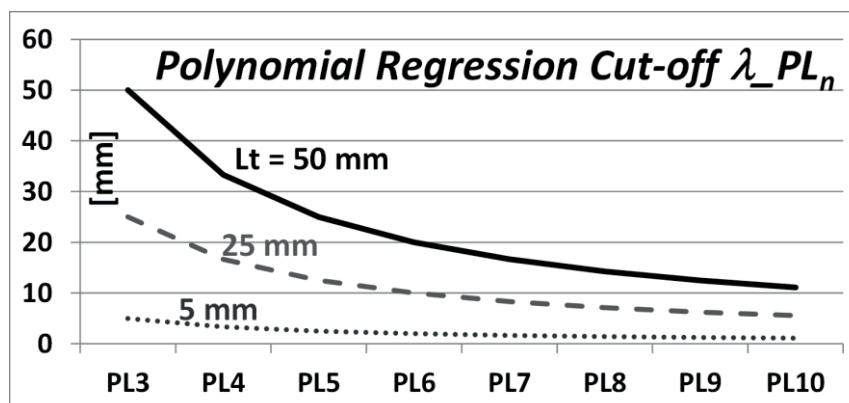


Fig. 10: Cut-off wavelength depending on the order of the fitted polynomial and the measuring length  $Lt$ , for different  $Lt$  values 50, 25 and 5 mm

For any profile of  $L_t = 50$  mm, a P5 polynomial (i.e. order 5) gives a cut-off value of  $\sim 25$  mm. This is remarkably in agreement with the naïve approach of “pseudo transmissions curves” as shown in Figure 8. The curves for  $L_t = 25$  mm and especially for 5 mm indicate that one should be careful in applying polynomial form removal on too short profiles. But of course this remark is equally valid for Gaussian filtering, where the cut-off value also has to be chosen carefully with respect to the measuring length.

#### 4. APPLICATION TO THE CARSTEEL WAVINESS GAUGE

The example given in section 3.1 is further used to quantitatively compare the polynomial regression with Gaussian filtering method for 2 different values of the form cut-off  $\lambda_f = 5$  mm and 10 mm, see Figure 11, left. It is clear and expectable that a cut-off  $\lambda_f = 5$  mm will heavily decrease the amplitude of the S3 component having a wavelength of 4.52 mm, being close to this cut-off value. This is of course a result of the shape of the Gaussian Filter. It is even more interesting to check the important influence of the 3 form removal methods on the final Wa-parameter itself: see Figure 11, right. One observes that the polynomial form removal is pretty close to the theoretical reference value, and even better than a Gaussian filtering with  $\lambda_f = 10$  mm.

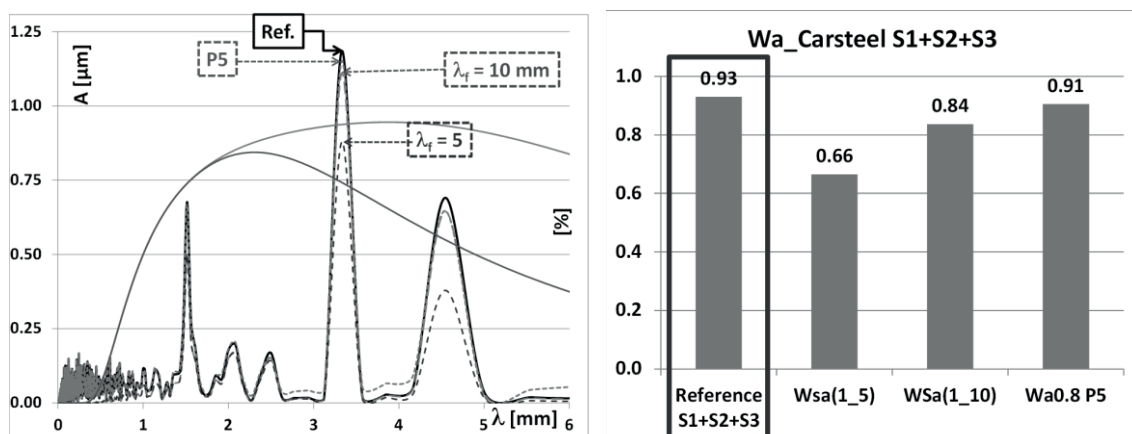


Fig. 11: Left: Reduction of the Fourier spectrum components for the CARSTEEL gauge profile, Right: Influence of the different approaches for form removal on the deviations from the theoretical Wa-parameter

#### 5. CONCLUSION

The industrial importance of paint quality perception has been evoked, as well as most influencing factors. Due to environmental and economic reasons, the waviness on the unpainted sheet metal becomes increasingly important, hence the need for a reliable and quantifiable waviness parameter. Such a parameter should remain unaffected by the roughness and by any shape, whether it is a bend in a laboratory sample or the intended (e.g. CAD) shape of a real component.

It was clearly demonstrated how classic polynomial regression can be formulated in terms of wavelengths or frequencies, through the use of the concept of Legendre polynomials. In this way one can use polynomial fitting as a valuable tool for form removal.

This approach was applied to the industrially relevant example of a physical waviness gauge as it was developed in the European CARSTEEL project. It was demonstrated that deviations from the theoretical value of the waviness parameter on this gauge, are acceptable when using a 5<sup>th</sup> order polynomial regression. These deviations are smaller than when a Gaussian band filtering is used even with a form cut-off of 10 mm.

## 6. REFERENCES

- [Dauser, 2013] Dauser, T.: Appearance Perception and Preference. Conference paper: European BYK-Gardner User Meeting 2013.
- [Deutscher, 2003] Deutscher, O.: Untersuchung über die Ursachen von längerwelligen Strukturanteilen in Feinblechoberflächen und deren Einflüsse auf das Lackierergebnis. Forschungsbericht P 402 der Studiengesellschaft Stahlanwendung e. V., 2003.
- [Deutscher, 2009] Deutscher, O.; Paesold, D.; et al.: Characterizing the surface waviness of hot dip galvanized steel sheets for optical high-quality paintability (CARSTEEL). ISBN 978-92-79-11303-1, European Communities, 2009.
- [Gerhardt, 2013] Gerhardt, L.: Global Competitive Benchmarking. Conference paper: US BYK-Gardner User Meeting 2013.
- [Kurzynski, 2015] Kurzynski, J.: Erarbeitung einer Normvorlage zur einheitlichen Bewertung des Einflusses der Welligkeit in der Feinblechoberfläche auf die Ausbildung der Decklack-Verlaufstruktur (WAVENORM). VDEh-Betriebsforschungsinstitut GmbH, 2015.
- [Meseure, 1996] Meseure, K; Scheers, J., et al.: Paint appearance in relation to surface topography. 3<sup>rd</sup> Sibetex Seminar, OCAS, 1996.
- [Schneider, 2013] Schneider, M.: Causes for the Formation of Surface Structures on Paint Films. Conference paper: European BYK-Gardner User Meeting 2013.
- [EN10049, 2013] EN10049:2013: Measurement of roughness average Ra and peak count R<sub>Pc</sub> on metallic flat products.
- [ISO16610-21, 2011] ISO 16610-21:2011: Geometrical product specifications, (GPS) – Filtration – Part 21: Linear profile filters: Gaussian filters.
- [SEP 1941, 2012] Messung des Welligkeitskennweters W<sub>sa</sub>(1-5) an kaltgewalzten Flacherzeugnisse. STAHL-EISEN Prüfblätter des Stahlinstituts VDEh, 2012.